Mineralogical Magazine, February 2018, Vol. 82(1), pp. 145–157

Fluoro-tremolite from the Limecrest-Southdown quarry, Sparta, New Jersey, USA: crystal chemistry of a newly approved end-member of the amphibole supergroup

Roberta Oberti[1,*], Fernando Cámara[2], Fabio Bellatreccia[3], Francesco Radica[3,4], Antonio Gianfagna[5] and Massimo Boiocchi[6]

[1] CNR-Istituto di Geoscienze e Georisorse, Sede secondaria di Pavia, via Ferrata 1, 27100 Pavia, Italy
[2] Dipartimento di Scienze della Terra "A. Desio", Università degli Studi di Milano, via Mangiagalli, 34, 20133 Milano, Italy
[3] Dipartimento di Scienze, Università Roma Tre, Largo San Leonardo Murialdo 1, 00146, Roma, Italy
[4] School of Science and Technology-Geology Division, University of Camerino, Via Gentile III da Varano, 62032 Camerino, Italy
[5] Dipartimento di Scienze della Terra, Università di Roma "La Sapienza", p.le Aldo Moro 5, 00185 Roma, Italy
[6] Centro Grandi Strumenti, Università di Pavia, via Bassi 21, 27100 Pavia, Italy

[*Received 20 March 2017; Accepted 25 April 2017; Associate Editor: Sergey Krivovichev*]

ABSTRACT

During systematic characterization of amphiboles that still lack a complete mineral description, fluoro-tremolite was identified in a specimen from the Limecrest-Southdown quarry, Sparta, New Jersey, USA, which was provided by the Franklin Mineral Museum. The ideal formula of fluoro-tremolite is $^{A}\square\ ^{B}Ca_2\ ^{C}Mg_5\ ^{T}Si_8O_{22}\ ^{W}F_2$ and the empirical formula derived for the holotype specimen, based on the results of electron-microprobe analysis and single-crystal structure refinement, is $^{A}(Na_{0.28}K_{0.02})_{\Sigma 0.30}\ ^{B}(Ca_{1.99}Na_{0.01})_{\Sigma 2.00}\ ^{C}(Mg_{4.70}Fe^{2+}_{0.28}Zn_{0.01}Ti^{4+}_{0.01})_{\Sigma 5.00}\ ^{T}(Si_{7.68}Al_{0.32})_{\Sigma 8.00}O_{22}\ ^{W}(F_{1.16}OH_{0.84})_{\Sigma 2.00}$. The unit-cell dimensions in space group $C2/m$ are $a = 9.846(2)$, $b = 18.050(3)$, $c = 5.2769(14)$ Å, $\beta = 104.80(2)°$ and $V = 906.7\ (3)$ Å^3 and $Z = 2$; the a:b:c ratio is 0.545:1:0.292. Fluoro-tremolite is biaxial (+), with $\alpha = 1.5987\ (5)$, $\beta = 1.6102(5)$, $\gamma = 1.6257(5)$, 2V(meas.) = 85(1)° and 2V(calc.) = 82°. The strongest ten reflections in the powder X-ray pattern [d values (in Å), I, (hkl)] are: 2.706, 100, (151); 3.126, 67, (310); 2.531, 59, ($\bar{2}02$); 3.381, 57, (131); 2.940, 43, ($\bar{1}51$, 221); 3.276, 37, (240); 2.337, 36, ($\bar{3}51$); 2.592, 35, (061); 2.731, 34, ($\bar{3}31$); 2.163, 34, (261). Both the mineral and the mineral name have been approved by the Commission on New Minerals, Nomenclature and Classification of the International Mineralogical Association (IMA2016–018); the holotype has been deposited at the Franklin Mineral Museum (32 Evans Street, Franklin, 07416 New Jersey, US), under the catalogue number 7710.

Comparison with new data on tremolite and synthetic fluoro-tremolite provides a more sound crystal-chemical model of the end-member compositions and their solid-solution.

Keywords: fluoro-tremolite, tremolite, amphibole, electron-microprobe analysis, crystal-structure refinement, Fourier-transform infrared spectroscopy, Limecrest-Southdown quarry.

Introduction

Fluoro-tremolite is the fluorine-analogue of tremolite, the composition at the root of amphibole compositional space in all classification schemes used to date.

According to the IMA list of minerals, (Pasero, 2018) the name tremolite was introduced to the mineralogical literature in 1789 (Höpfner, 1789) and the name has been grandfathered into all nomenclature schemes. The structure of tremolite was solved by Warren (1929). Structural data were first provided

*E-mail: oberti@crystal.unipv.it
https://doi.org/10.1180/minmag.2017.081.029

by Papike *et al.* (1969) on tremolite from the Gouverneur mining district, NewYork. However, due to the extensive presence of inclusions and exolution, these data should be considered with some caution. The structural reference data to date were provided by Hawthorne and Grundy (1976) for a sample that has $F^{-}_{0.66}$ per formula unit (pfu). Because F^{-} occurs at the O(3) site, which is coordinated by the cations occurring at the *M*(1) and *M*(3) sites, these authors observed a significant shortening of the <*M*(1)–O> and <*M*(3)–O> distances.

Despite the frequent use of the term 'fluoro-tremolite' (and its spelling variants: 'fluorotremo-lite and 'fluortremolite') in the mineralogical literature (e.g. Valley *et al*., 1982; Petersen *et al*., 1982; Dachs *et al*., 2010), this still has remained a *named* amphibole (Burke and Leake, 2004) and lacked a complete mineralogical description.

Structural data of natural and synthetic tremolite crystals started being reported in the 1970s; structural data for synthetic fluoro-tremolite were first reported by Cameron and Gibbs (1973), who showed that the substitution of F^{-} for $(OH)^{-}$ significantly reduces the size of the strip of octahedra and hence the *a* and *b* cell parameters. The higher thermal stability of fluoro-tremolite was explained both by the higher bond-strength of the Mg–F bonds, and by the loss of local electroneutrality due to the thermal instability of the O–H bond and the subsequent H loss at high temperature, which cannot be balanced by oxidation of divalent cations at the *M*(1) and *M*(3) sites.

In this paper, we provide a complete mineral description of fluoro-tremolite from the Limecrest-Southdown quarry, Sparta, New Jersey, USA, which was kindly provided by the Franklin Mineral Museum. We also provide new structure and crystal-chemical data for synthetic fluoro-tremolite (code 751 in the amphibole database of the CNR-IGG in Pavia, Italy) and tremolite from the type locality of Val Tremola (code 361 in the amphibole database of the CNR-IGG).

Mineral data

Occurrence and type material

The sample comes from the skarns at the Limecrest-Southdown quarry, Sparta, New Jersey, USA. It was provided by John Cianciulli, the former curator of the Franklin Mineral Museum (32 Evans Street, Franklin, 07416 New Jersey, USA) and is labelled G409. Co-existing phases in the holotype are: calcite, chondrodite and pyrrhotite. The refined and analysed crystal of this work was assigned code 1082 in the amphibole database of the CNR-IGG.

The new mineral and its name have been approved by Commission on New Minerals, Nomenclature and Classification of the International Mineralogical Association (IMA2016-018). Holotype material has been deposited at the Franklin Mineral Museum under the catalogue number 7710.

Appearance, physical and optical properties

Fluoro-tremolite occurs as prismatic light-greenish to colourless crystals forming grey to whitish green aggregates. It has a grey streak and vitreous lustre; the crystals are transparent and do not fluoresce under ultraviolet illumination. Based on the unit-cell parameters and the empirical formula, the calculated density is 3.044 g cm^{-3}.

Fluoro-tremolite is biaxial (+), with $\alpha = 1.5987(5)$, $\beta = 1.6102(5)$, $\gamma = 1.6257(5)$ (589 nm) $2V_z$(meas.) = 85(1)° and $2V_z$(calc.) = 82°. Refractive indexes were determined by the double-variation method (Su *et al*., 1987, Gunter *et al*., 2005) using standard Cargille liquids.

Crystallography

For holotype fluoro-tremolite and for the other crystals reported in this work, single-crystal diffraction data were collected in the θ range 2–30° with a Philips PW1100 diffractometer working with graphite monochromatized Mo*K*α X-radiation (λ = 0.7107 Å). Unit-cell parameters were calculated by a least-squares procedure using the *d** values measured for reflections belonging to 60 selected rows of reciprocal space and occurring in the θ range –30 to +30°.

Two sets of monoclinic equivalents (*hkl* and *h*–*kl*) were collected. Intensities were corrected for Lorentz and polarization effects and for absorption and then merged. The reflections with $Io > 3\sigma(I)$ were considered as observed during unweighted full-matrix least-squares refinement on *F*. Scattering curves for fully ionized chemical species were used at sites where chemical substitutions occur; neutral versus ionized scattering curves were refined for the *T* and anion sites [except O(3)] in the full-matrix least-squares refinement on $I > 3\sigma(I)$. The relevant crystallographic details are reported in Table 1. Atom coordinates, site-scattering values and anisotropic-displacement parameters resulting from the structure refinement are given in Table 2, and selected interatomic distances and angles are given in Table 3. The crystallographic information files with embedded structure factors are available as supplementary material (see below).

TABLE 1. Unit-cell parameters and crystallographic details for holotype fluoro-tremolite (1082)*, new refinements of synthetic fluoro-tremolite (751) and tremolite (361) provided in this work, and a comparison with those reported by Hawthorne and Grundy (1976) for $^{A}(Na_{0.192}K_{0.118})^{B}(Na_{0.191}Ca_{1.809})^{C}(Mg_5)^{T}(Al_{0.228}Si_{7.767})O_{22}{}^{W}(OH_{1.337}F_{0.660}Cl_{0.012})$.

	1082	751	361	H&G**
a (Å)	9.846(2)	9.784(2)	9.8359(3)	9.863(1)
b (Å)	18.050(3)	18.015(4)	18.0450(6)	18.048(2)
c (Å)	5.2769(14)	5.272(2)	5.2752(2)	5.285(1)
β (°)	104.80(2)	104.52(2)	104.750(3)	104.79(1)
V (Å^3)	906.7(3)	899.6(4)	905.44(5)	909.6(2)
θ range (°)	2–30	2–30	2–30	2–32.5
Space group (*Z* = 2)	*C*2/*m*	*C*2/*m*	*C*2/*m*	*C*2/*m*
Size (μm)	400 × 230 ×130	460 × 260 × 230	330 × 160 × 80	260 × 150 × 50
Scan width (°)	2.4	2.1	2.4	2.0
Scan speed (°s^{-1})	0.04	0.12	0.08	0.033–0.4
R_{sym} %	1.2	2.2	1.4	n.r.
R_{obs} %	1.3	1.7	1.7	3.2
R_{all} %	1.7	3.3	2.0	4.4
# all	1373	1368	1367	1640
# obs	1229	1007	1263	1376

n.r. = not reported; *Specimen numbers in the amphibole database of CNR-IGG; **H&G = Hawthorne and Grundy (1976).

Powder X-ray diffraction data (Cu*K*α, λ = 1.54178 Å) for holotype fluoro-tremolite were obtained using the *XPREP* utility of *SAINT* (Bruker, 2003), which generates a 2D powder diffractogram (Debye-Scherrer technique) starting from the F_{obs} collected on a second single-crystal and taking into account solely the information concerning the unit-cell parameters (ucp) and the Laue symmetry. No Lorentz and polarization corrections were applied. Powder X-ray-diffraction data are given in Table 4. In order to check its composition, diffraction data for the second crystal were collected in the diffraction lab of the CrisDi (University of Torino) with an Oxford Gemini R Ultra diffractometer equipped with a CCD area detector and working with graphite-monochromatized Mo*K*α radiation (λ = 0.7107 Å). The unit-cell parameters are: *a* = 9.8423(4) Å, *b* = 18.0613(5) Å, *c* = 5.2737(2) Å, β = 104.693(4)° and *V* = 906.81(6) Å^3, and the structure refinement is almost indistinguishable from that of the analysed crystal 1082 (and therefore is not reported in the following tables).

Empirical formula

Chemical analyses (3 analytical points) were obtained for crystal 1082 using a Cameca SX50 at Istituto di Geologia Ambientale e Geoingegneria (IGAG), Università di Roma "La Sapienza". Analytical conditions were 15 kV accelerating voltage and 15 nA beam current, with a 5 μm beam diameter. Counting time was 20 s on both peak and background. Analytical errors are 1% rel. except for fluorine which is estimated to be 3% rel. Standards, spectral lines, and crystals used were: wollastonite (Si*K*α, Ca*K*α, PET), rutile (Ti*K*α, LIF), corundum (Al*K*α, TAP), magnetite (Fe*K*α, LIF), Mn metal (Mn*K*α, LIF), Zn metal (Zn*K*α, LIF), Cr metal (Cr*K*α, PET), periclase (Mg*K*α, TAP), jadeite (Na*K*α, TAP), orthoclase (K*K*α, PET), synthetic fluor-phlogopite (F*K*α, TAP) and sylvite (Cl*K*α, PET). Data reduction was done by the *PAP* method (Pouchou and Pichoir, 1985). The H_2O content was calculated by stoichiometry (F+OH+Cl = 2 atoms per formula unit (apfu)), taking into account the total number of cations obtained by structure refinement. Analytical data are given in Table 5. The empirical formula (based on 24 anions pfu) is $^{A}(Na_{0.28}K_{0.02})_{\Sigma 0.30}$ $^{B}(Ca_{1.99}Na_{0.01})_{\Sigma 2.00}$ $^{C}(Mg_{4.70}Fe^{2+}_{0.28}Zn_{0.01}Ti^{4+}_{0.01})_{\Sigma 5.00}$ $^{T}(Si_{7.68}Al_{0.32})_{\Sigma 8.00}$ O_{22} $^{W}(F_{1.16}OH_{0.84})_{\Sigma 2.00}$. The ideal formula for end-member fluoro-tremolite (Hawthorne *et al.*, 2012) is $^{A}\square$ $^{B}Ca_2$ $^{C}Mg_5$ $^{T}Si_8$ O_{22} $^{W}F_2$, which requires SiO_2 58.88, MgO 24.68, CaO 13.74, F 4.65, –F=O –1.95, total 100.00 wt.%.

The compatibility index [$1 - (K_p/K_c)$; Mandarino, 1981] is 0.010 (superior).

TABLE 2. Refined site-scattering values (ss, electrons per formula unit), fractional atom coordinates and atom-displacement parameters (B_{eq}, Å^2; β^{ij} x 10^4) for holotype fluoro-tremolite (crystal 1082) and the other samples described in this work.

Site	ss	*x/a*	*y/b*	*z/c*	B_{eq}	β^{11}	β^{22}	β^{33}	β^{12}	β^{13}	β^{23}
Fluoro-tremolite Limecrest-Southdown quarry 1082											
O(1)		0.11158(7)	0.08528(4)	0.21841(14)	0.50(2)	13	4	50	0	7	−1
O(2)		0.11900(7)	0.17061(4)	0.72473(14)	0.52(2)	12	5	50	−1	7	0
O(3)	17.36(2)	0.10575(10)	0	0.7142(2)	0.73(2)	23	5	65	–	10	–
O(4)		0.36471(8)	0.24827(4)	0.79183(14)	0.68(2)	22	4	68	−3	13	−2
O(5)		0.34727(8)	0.13502(4)	0.10136(14)	0.70(2)	16	7	60	0	6	7
O(6)		0.34476(8)	0.11829(4)	0.59230(14)	0.68(2)	16	6	60	0	8	−6
O(7)		0.33989(11)	0	0.2908(2)	0.78(2)	19	4	106	–	10	–
T(1)		0.28110(3)	0.08396(2)	0.29806(5)	0.36(2)	10	3	36	−1	5	−1
T(2)		0.28889(3)	0.17117(2)	0.80540(5)	0.38(2)	10	3	35	−1	5	0
M(1)	25.04(6)	0	0.08816(3)	½	0.49(2)	15	4	46	–	9	–
M(2)	26.24(6)	0	0.17652(2)	0	0.46(2)	13	3	45	–	8	–
M(3)	12.42(3)	0	0	0	0.49(2)	15	3	42	–	5	–
M(4)	39.00(8)	0	0.27804(2)	½	0.70(2)	24	4	82	–	28	–
M(4′)	1.10(5)	0	0.2616(7)	½	0.8(2)						
A	0.70(2)	0	½	0	1.6(5)	51	14	137	–	42	–
A(*m*)	1.87(7)	0.0451(14)	½	0.104(3)	2.1(3)	34	28	153	–	30	–
A(2)	0.79(7)	0	0.4721(11)	0	2.0(7)	55	7	385	–	132	–
H	0.98(8)	0.195(5)	0	0.762(9)	1.0						
Synthetic fluoro-tremolite 751											
O(1)		0.11235(11)	0.08489(6)	0.2178(2)	0.48(2)	13	4	49	0	6	−1
O(2)		0.11921(11)	0.17018(6)	0.7240(2)	0.53(2)	15	4	46	−1	5	0
O(3)	17.98(3)	0.10271(14)	0	0.7122(3)	0.63(3)	20	4	60	–	9	–
O(4)		0.36560(12)	0.24852(6)	0.7896(2)	0.79(2)	27	4	72	−4	4	−1
O(5)		0.34821(11)	0.13531(6)	0.0995(2)	0.75(2)	18	7	64	−1	6	7
O(6)		0.34599(11)	0.11881(6)	0.5882(2)	0.75(2)	16	7	68	0	5	−7
O(7)		0.3417(2)	0	0.2895(3)	0.84(4)	17	4	127	–	14	–
T(1)		0.28299(4)	0.08376(2)	0.29630(8)	0.40(2)	11	3	42	−1	5	−1
T(2)		0.29013(4)	0.17084(2)	0.80332(8)	0.44(2)	13	3	37	−1	4	0
M(1)	24.0(2)	0	0.08815(4)	½	0.47(2)	15	4	38	–	5	–
M(2)	24.1(2)	0	0.17631(4)	0	0.44(3)	15	3	36	–	7	–
M(3)	11.99(8)	0	0	0	0.46(5)	14	3	41	–	5	–
M(4)	36.69(13)	0	0.27717(4)	½	0.76(2)	25	5	86	–	31	–
M(4′)	1.56(5)	0	0.2492(9)	½	0.3(2)						
A(*m*)	1.48(8)	0.049(2)	½	0.113(4)	2.5(3)						
A(2)	1.04(8)	0	0.4780(13)	0	2.2(4)						

Tremolite Val Tremola 361											
O(1)		0.11168(10)	0.08595(6)	0.2176(2)	0.46(2)	10	4	51	0	5	0
O(2)		0.11855(10)	0.17106(6)	0.7242(2)	0.50(2)	11	4	55	0	6	−1
O(3)		0.1097(2)	0	0.7155(3)	0.55(3)	14	4	59	–	6	–
O(4)		0.36527(11)	0.24795(6)	0.7931(2)	0.62(2)	19	4	69	−2	12	−1
O(5)		0.34630(11)	0.13424(6)	0.1000(2)	0.57(2)	13	6	48	−1	4	5
O(6)		0.34370(11)	0.11863(6)	0.5892(2)	0.57(2)	14	6	44	0	5	−6
O(7)		0.3372(2)	0	0.2922(3)	0.65(3)	16	2	99	–	9	–
T(1)		0.28025(4)	0.08401(2)	0.29701(8)	0.34(2)	9	2	33	0	3	0
T(2)		0.28829(4)	0.17113(2)	0.80461(8)	0.35(2)	9	3	31	−1	3	0
M(1)	24.00(8)	0	0.08773(4)	½	0.41(2)	13	3	40	–	6	–
M(2)	24.00(8)	0	0.17654(4)	0	0.40(2)	11	3	43	–	6	–
M(3)	12.00(4)	0	0	0	0.39(2)	11	3	38	–	4	–
M(4)	39.93(13)	0	0.27788(2)	½	0.61(2)	20	4	72	–	22	–
H	2.00	0.190(5)	0	0.780(9)	3.9(10)						

TABLE 3. Selected interatomic distances (Å) and angles (°) in holotype fluoro-tremolite 1082 and in the other crystals of this work.

	1082	751	361		1082	751	361
T(1)–O(1)	1.6140(8)	1.6163(12)	1.6038(11)	*M*(4′)–O(2) ×2	2.183(9)	2.023(12)	
T(1)–O(5)	1.6422(8)	1.6364(12)	1.6334(11)	*M*(4′)–O(4) ×2	2.286(13)	2.2513(13)	
T(1)–O(6)	1.6403(9)	1.6346(13)	1.6327(11)	*M*(4′)–O(5) ×2	2.925(8)	3.069(12)	
T(1)–O(7)	1.6262(5)	1.6181(8)	1.6184(7)	*M*(4′)–O(6) ×2	2.767(9)	2.914(14)	
<*T*(1)–O>	1.6307	1.6264	1.6221	<*M*(4′)–O>	2.540	2.564	
T(2)–O(2)	1.6173(8)	1.6188(12)	1.6145(11)	*A*–O(5) ×4	2.9829(9)		
T(2)–O(4)	1.5895(8)	1.5924(12)	1.5881(11)	*A*–O(6) ×4	3.1374(9)		
T(2)–O(5)	1.6543(8)	1.6512(13)	1.6564(11)	*A*–O(7) ×2	2.4649(12)		
T(2)–O(6)	1.6716(8)	1.6655(13)	1.6737(11)	<*A*–O>	2.9411		
<*T*(2)–O>	1.6332	1.6320	1.6332	*A*(*m*)–O(5) ×2	3.118(8)	3.118(12)	
M(1)–O(1) ×2	2.0620(8)	2.0606(12)	2.0640(10)	*A*(*m*)–O(5) ×2	2.970(8)	2.963(11)	
M(1)–O(2) ×2	2.0698(8)	2.0610(12)	2.0777(11)	*A*(*m*)–O(6) ×2	2.724(8)	2.705(12)	
M(1)–O(3) ×2	2.0720(7)	2.0542(10)	2.0828(10)	*A*(*m*)–O(7)	2.464(13)	2.43(2)	
<*M*(1)–O>	2.0679	2.0586	2.0748	*A*(*m*)–O(7)	3.105(14)	3.06(2)	
M(2)–O(1) ×2	2.1449(9)	2.1461(13)	2.1341(12)	*A*(*m*)–O(7)	2.613(13)	2.61(2)	

(continued)

TABLE 3. (*contd*.)

	1082	751	361		1082	751	361
M(2)–O(2) ×2	2.0890(8)	2.0836(12)	2.0859(10)	<*A*(*m*)–O>	2.867	2.85	
M(2)–O(4) ×2	2.0191(8)	2.0154(13)	2.0168(11)	*A*(2)–O(5) ×2	2.59(2)	2.65(2)	
<*M*(2)–O>	2.0843	2.0817	2.0789	*A*(2)–O(6) ×2	2.819(12)	2.896(14)	
M(3)–O(1) ×4	2.0634(7)	2.0573(11)	2.0707(10)	*A*(2)–O(7) ×2	2.516(4)	2.464(4)	
M(3)–O(3) ×2	2.0397(10)	2.0190(14)	2.059(2)	<*A*(2)–O>	2.64	2.67	
<*M*(3)–O>	2.0555	2.0445	2.067	O(3)–H	0.85(5)		0.77(5)
M(4)–O(2) ×2	2.4144(9)	2.4039(13)	2.4024(11)	*T*(1)–O(5)–*T*(2)	136.03(5)	136.32(7)	136.39(7)
M(4)–O(4) ×2	2.3280(9)	2.2980(13)	2.3253(10)	*T*(1)–O(6)–*T*(2)	137.78(5)	138.40(7)	138.19(7)
M(4)–O(5) ×2	2.7447(9)	2.7526(14)	2.7621(11)	*T*(1)–O(7)–*T*(1)	137.47(7)	137.66(11)	139.00(10)
M(4)–O(6) ×2	2.5408(8)	2.5199(13)	2.5379(11)	O(5)–O(6)–O(5)	166.90(5)	167.09(7)	167.76(6)
<*M*(4)–O>	2.5070	2.4936	2.5069	O(6)–O(7)–O(6)	107.01(5)	107.64(8)	108.13(7)

TABLE 4. Calculated powder X-ray data for holotype fluoro-tremolite.

I_{rel}	*d*(calc)	*h k l*	I_{rel}	*d*(calc)	*h k l*	I_{rel}	*d*(calc)	*h k l*	I_{rel}	*d*(calc)	*h k l*
16.64	5.092	0 0 1	11.38	2.807	3 3 0	8.68	2.208	$\bar{2}$ 4 2	12.49	1.865	$\bar{1}$ 9 1
		1 3 0	**33.94**	**2.731**	**$\bar{3}$ 3 1**	8.42	2.181	1 7 1	6.34	1.843	$\bar{1}$ 7 2
32.38	4.875	$\bar{1}$ 1 1	**100.00**	**2.706**	**1 5 1**	**33.50**	**2.163**	**2 6 1**	5.93	1.746	$\bar{5}$ 1 2
24.20	4.515	0 4 0	**34.49**	**2.592**	**0 6 1**	6.79	2.143	$\bar{3}$ 3 2	15.93	1.684	$\bar{2}$ 8 2
8.47	4.211	2 2 0	**59.36**	**2.531**	**$\bar{2}$ 0 2**	16.13	2.043	2 0 2			$\bar{1}$ 3 3
23.66	3.875	$\bar{1}$ 3 1	7.58	2.411	$\bar{2}$ 6 1	22.54	2.016	3 5 1	8.17	1.671	0 2 3
56.74	**3.381**	**1 3 1**	8.47	2.384	3 5 0			$\bar{4}$ 0 2	24.78	1.650	4 6 1
37.52	**3.276**	**2 4 0**	**35.85**	**2.337**	**$\bar{3}$ 5 1**	10.45	2.003	3 7 0	9.53	1.638	4 8 0
66.66	**3.126**	**3 1 0**	21.25	2.323	$\bar{4}$ 2 1	7.58	1.964	1 9 0	12.89	1.618	1 11 0
43.08	**2.940**	**$\bar{1}$ 5 1**	20.06	2.299	$\bar{1}$ 7 1	5.13	1.935	$\bar{3}$ 5 2	6.88	1.586	6 0 0
		2 2 1	21.98	2.274	$\bar{3}$ 1 2	8.66	1.894	5 1 0	22.58	1.577	$\bar{1}$ 5 3
									6.43	1.555	4 0 2

The strongest ten reflections are in bold.

TABLE 5. Chemical composition and unit formula (atoms per formula unit, apfu) calculated based on 24 (O, OH, F) apfu for holotype fluoro-tremolite (crystal 1082) and in the other crystals of this work.

Oxide	wt.%	Range	Oxide	wt.%	Range		apfu		apfu
1082									
SiO_2	55.52(13)	55.40–55.66	Na_2O	1.10(5)	1.06–1.16	Si	7.68	Na	0.01
TiO_2	0.14(7)	0.07–0.21	K_2O	0.11(1)	0.11–0.13	Al	0.32	Ca	1.99
Al_2O_3	1.95(12)	1.86–2.09	H_2O*	0.91		Sum T	8.00	Sum B	2.00
Cr_2O_3	0.02(2)	0.00–0.05	F	2.65(12)	2.52–2.76	Ti^{4+}	0.01	Na	0.28
FeO_{tot}	2.44(7)	2.37–2.51	Cl	0.03(1)	0.02–0.04	Mg	4.70	K	0.02
MnO	0.03(5)	0.00–0.08	O=F	−1.11		Fe^{2+}	0.28	Sum A	0.30
MgO	22.74(18)	22.54–22.88	O=Cl	−0.01		Zn	0.01	F^-	1.16
ZnO	0.10(17)	0.00–0.29	Total	100.03		Sum C	5.00	$(OH)^-$	0.84
CaO	13.41(9)	13.34–13.51						Sum W	2.00

Oxide	wt.%		apfu		apfu	Oxide	wt.%		apfu		apfu
751						**361**					
SiO_2	56.77	Si	7.78	Mg	0.25	SiO_2	59.12	Si	8.00	$(OH)^-$	2.00
Al_2O_3	1.66	Al	0.22	Ca	1.75	FeO_{tot}	0.38	Sum T	8.00	Sum W	2.00
MgO	25.43	Sum T	8.00	Sum B	2.00	MnO	0.02	Mg	5.00		
CaO	12.50	Al^{3+}	0.05	Ca	0.09	CaO	13.48	Sum C	5.00		
F	4.59	Mg	4.95	Sum A	0.09	MgO	24.78	Fe^{2+}	0.04		
O=F	–1.93	Sum C	5.00	F^-	1.99	H_2O*	2.22	Ca	1.96		
Total	99.02			Sum W	1.99	Total	100.00	Sum B	2.00		

* calculated based on single-crystal structure-refinement results and with the constraints of non-negative Fe^{2+} values and ^{W}(OH, F, Cl) = 2 apfu.

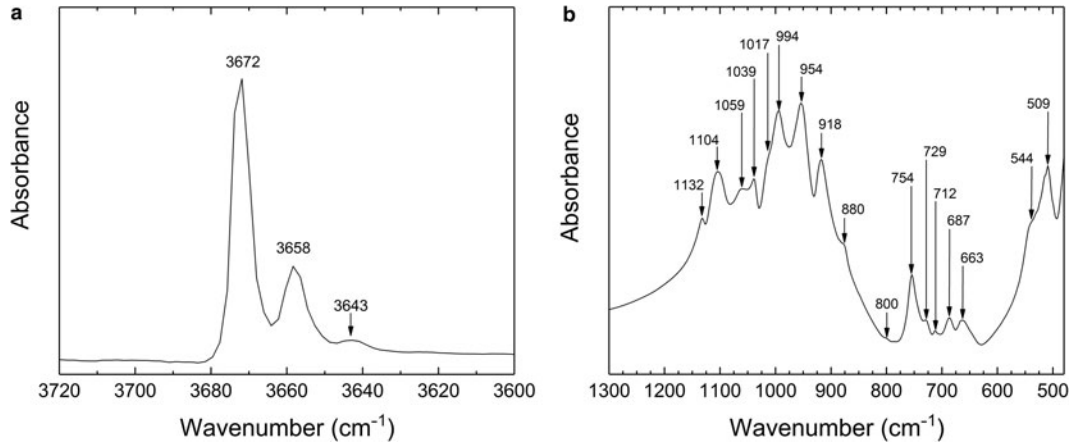

FIG. 1. FTIR spectra of fluoro-tremolite: (*a*) region of the absorptions due to OH-stretching, (*b*) region of the absorptions due to structural vibrations.

TABLE 6. Position (cm^{-1}) and assignments of the bands in the FTIR spectra of fluoro-tremolite.

OH Stretching region		Assignment*
A	3672 p	MgMgMg–OH–$^{A}\square$:SiSi
B	3658 p	MgMgFe^{2+}–OH–$^{A}\square$:SiSi or MgMgMg–OH/F–$^{A}\square$:SiSi
C	3643 p	MgFe^{2+}Fe^{2+}–OH–$^{A}\square$:SiSi or MgMgMg–OH–$^{A}\square$:AlSi
Region 1		
E	1132 p	Si–O stretching
F	1104 p	
G'	1059 p	
G	1039 p	
H'	1017 sh	
H	994 p	
I	954 p	
J	918 p	
I'	880 sh	$^{[4]}$Al–O
J'	800 sh	
Region 2		
K	755 p	Si–O–Si deformation
L		
n.r.		
M	729 p	
K'	712 p	Si–O–$^{[4]}$Al deformation
N	687 p	O–H libration
O	663 p	O–Si–O deformation
P		n.r.
Region 3		
Q	544 sh	M–O deformation
R	509 p	

* Assignments and letters for the absorptions in regions 1, 2 and 3 from Ishida *et al.* (2008).
p: resolved peak; sh: shoulder; n.r.: not resolved.

Fourier-transform infrared spectroscopy

The powder Fourier-transform infrared (FTIR) spectra were collected at the Dipartimento di Scienze, Università Roma Tre on a Nicolet Magna 760 FTIR spectrometer equipped with a DTGS detector and a KBr beamsplitter; the nominal resolution was 4 cm^{-1} and 64 scans were averaged for each sample and for the background. The spectra were collected from KBr disks with ~7 mg of sample in 150 mg of KBr for the 3600–3720 cm^{-1} region, and 3.5 mg of sample in 150 mg of KBr for the 550–2000 cm^{-1} region. The FTIR spectrum in the OH-stretching region (Fig. 1*a*) shows only two well-resolved peak at 3672 cm^{-1} and 3658 cm^{-1} and one broad and very weak band at 3643 cm^{-1}. The spectral range from 1200 to 400 cm^{-1}, typical of lattice vibrations, can be divided in three regions, which are characterized by the occurrence of three multicomponent absorptions (Fig. 1*b* and Table 6). Region 1 (1200–800 cm^{-1}) shows ten strong bands or shoulders, region 2 (800–630 cm^{-1}) shows five weaker absorptions, and region 3 (600–550 cm^{-1}) shows one very strong absorption at 509 cm^{-1} with a pronounced shoulder at 544 cm^{-1}.

Discussion and concluding remarks

Site populations for crystal 1082 were derived from the unit-formula and the results of the structure refinement. They are reported in Table 7.

As expected from the current knowledge of amphibole crystal-chemistry (cf. the review of Oberti *et al.*, 2007), $^{C}Fe^{2+}$ has the following (weak) site preference: $M(2)>M(1)>M(3)$. As expected for a fluorine-rich amphibole, the A cations preferentially order at the $A(m)$ subsite where Coulombic interactions with F^- are stronger.

Contrary to what is expected as a result of the presence of F^- at the O(3) site, the $M(1)$–O(3) distance for fluoro-tremolite 1082 is the longest in the $M(1)$ octahedron, whereas the $M(3)$–O(3) distance is the shortest in the $M(3)$ octahedron (and much shorter than expected), suggesting a relaxation pattern peculiar to this composition. This pattern is more evident if individual $M(1,3)$–O distances are compared as a function of F^- content (Fig. 2). In fact, although the $M(1)$–O(3) distance is the longest of the $M(1)$ polyhedron in tremolite 361 and in fluoro-tremolite 1082, it is the shortest in synthetic fluoro-tremolite 751, where it is 2.054(1) Å (Table 3). Therefore, complete $^{O(3)}(OH)_{-1}{}^{O(3)}F_1^-$ substitution appears to result in a reduction of this distance of 0.028 Å, i.e. ~1.4%, half of what is expected based on the ionic radii for $(OH)^-$ and F^- in 4-coordination (1.35 and 1.31 Å, respectively; Shannon, 1976). A somewhat stronger shortening is observed for the $M(3)$–O(3) distance (Δ = –0.040 Å, ≈ 1.9%). Sample 1082 plots slightly above the line in Fig. 2 because of its small Fe^{2+} content. The significant contraction observed for the $M(1)$–O(2) and $M(3)$–O(1) bond distances deserves comment: although the O(1) and O(2) sites are not involved in the $^{O(3)}(OH)_{-1}{}^{O(3)}F_1^-$ exchange, complete substitution of $(OH)^-$ by F^- produces a decrease of 0.017 Å and 0.013 Å for the $M(1)$–O(2) and $M(3)$–O(1) bond distances,

TABLE 7. Site population for fluoro-tremolite 1082. There is a good agreement between the refined values of site-scattering (ss, electrons per formula unit) and mean bond-lengths (mbl, Å) and those calculated based on the proposed site populations.

		ss (epfu)		mbl (Å)	
Site	Site population (apfu)	Refined	Calculated	Refined	Calculated
$T(1)$	3.68 Si^{4+} + 0.32 Al^{3+}			1.631	1.629
$T(2)$	4 Si^{4+}				
$M(1)$	1.91 Mg^{2+} + 0.09 Fe^{2+}	25.04	25.26	2.068	2.065
$M(2)$	1.83 Mg^{2+} + 0.15 Fe^{2+}+ 0.01 Zn + 0.01 Ti^{4+}	26.24	26.38	2.084	2.081
$M(3)$	0.96 Mg^{2+} + 0.04 Fe^{2+}	12.42	12.56	2.055	2.065
Σ C cations		63.70	64.20		
B cations	1.99 Ca^{2+} + 0.01 Na	40.10	39.91		
A cations	0.28 Na^+ + 0.02 K^+	3.36	3.46		
W anions	1.16 F^- + 0.84 $(OH)^-$	17.36	17.16		

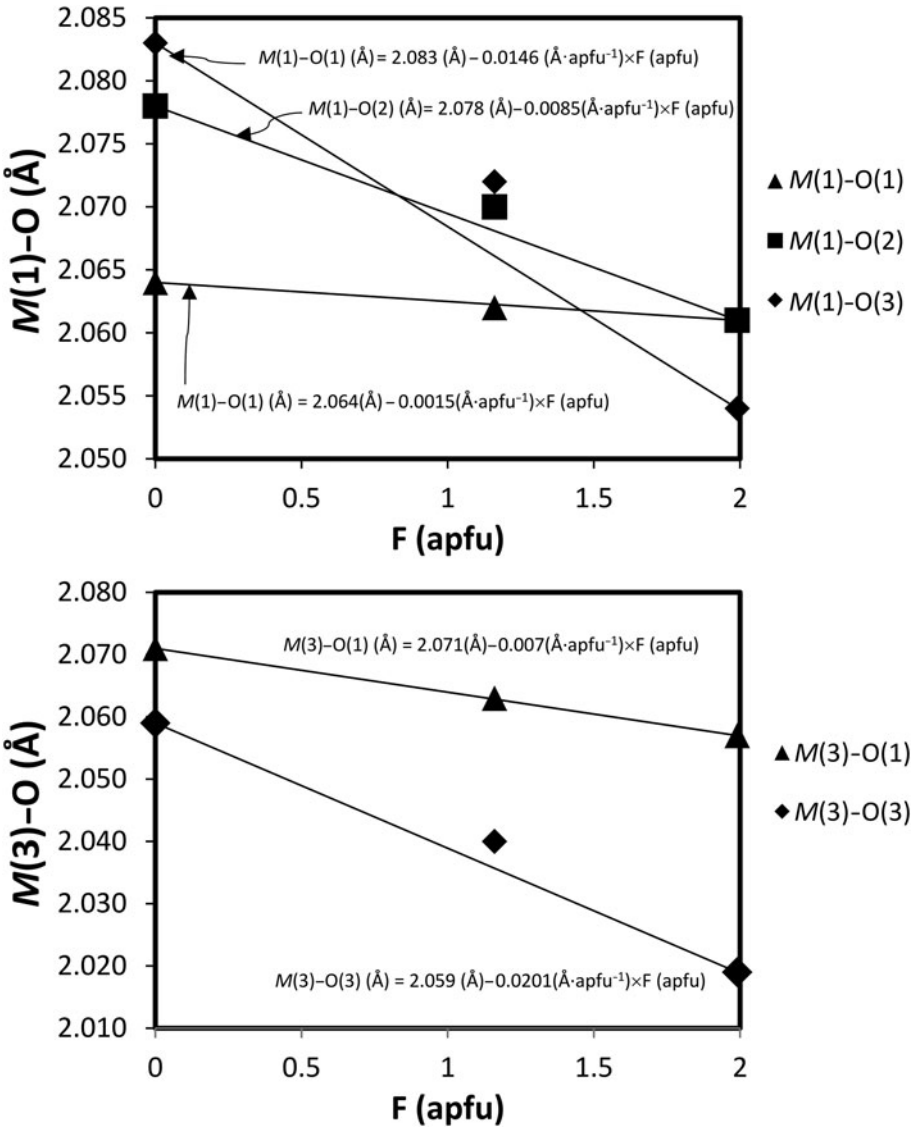

FIG. 2. Changes in the individual *M*(1,3)–O bond distances as a function of the F content in the samples studied. Errors are within symbol size. Equations give the slopes of the lines joining the geometries of the end-member compositions. Sample 1082 plots above the lines due its low but significant Fe^{2+} content, which enlarges the *M*(1) and *M*(3) polyhedra.

respectively. This shortening must be related to a general contraction of the O-layer due to the presence of F^- at the O(3) site, as shown in Fig. 3. With complete $^{O(3)}(OH)_{-1}{}^{O(3)}F^-_1$ substitution, the O(3)–O(1) and O(3)–O(2) distances shorten by 0.068 Å and 0.018 Å, respectively, and this change is coupled to a small but significant increase of the rotation of the double chain of tetrahedra (the angle *T*(1)–O(7)–*T*(1) shrinks by 1.3°). Interestingly, at the *M*(2) site, complete $^{O(3)}(OH)_{-1}{}^{O(3)}F^-_1$ substitution produces a significant increase of the *M*(2)–O(1) distance (by 0.012 Å).

The FTIR spectrum of fluoro-tremolite 1082 is quite similar to that reported for synthetic fluoro-tremolite (1.9 F^- apfu) by Ishida *et al.* (2008). Differences can be related to the more complex

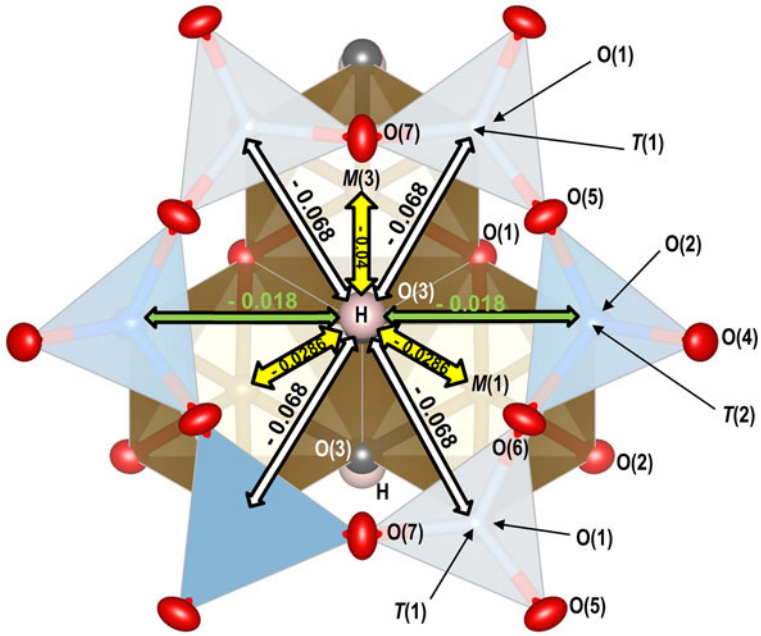

FIG. 3. The local environment of the O(3) site: the arrows show the shortening of the O(3)–O(1) (white) and O(3)–O(2) edges (green) and of the *M*(1,3)–O(3) bond distances (yellow) passing from tremolite 361 to synthetic fluoro-tremolite 751 (i.e. for complete $^{O(3)}(OH)_{-1}{}^{O(3)}F_1^-$ substitution).

composition of the mineral. In the region of the OH-stretching vibrations, the band at 3672 cm^{-1} can be assigned to the local arrangement MgMgMg–OH–$^{A}\square$:SiSi characteristic of end-member tremolite. Its position was 3675 cm^{-1} in the tremolite with 0.66 F^- apfu studied by Hawthorne *et al.* (2000). The other absorptions at 3658 cm^{-1} and 3643 cm^{-1} might be assigned, respectively, to the arrangements MgMgFe–OH–$^{A}\square$:SiSi and MgFeFe–OH–$^{A}\square$:SiSi (Burns and Strens, 1966; Hawthorne *et al.*, 2007). However, considering the low Fe^{2+} content at the *M*(1) and *M*(3) sites and the presence of 0.32 apfu of Al at the *T*(1) site (Table 7), these assignments may not be correct. In fact, the substitution of Al for Si lowers the frequency of the OH absorption (~25 cm^{-1}), so that the weak band at 3643 cm^{-1} can be better assigned to the MgMgMg-OH-$^{A}\square$:AlSi arrangement (Hawthorne *et al.*, 1996, 2000).

Another interesting feature is the lack of absorptions at frequencies higher than 3672 cm^{-1}, typical of *A*-site-filled arrangements, notwithstanding the presence of 0.30 apfu of A cations. The low band intensity, which is due to the presence of only 0.84 $(OH)^-$ apfu is not a satisfactory explanation. We infer complete local coupling of A cations with $^{O(3)}F^-$, as confirmed by the shape of the electron density, which is consistent with their order at the *A*(*m*) subsite closer to O(3) (cf. Hawthorne *et al.*, 1996). A further consideration may be applied to the band at 3658 cm^{-1}. A downward shift of the OH-band by 15–18 cm^{-1} due to the $^{O(3)}(OH)_{-1}{}^{O(3)}F_1^-$ exchange has been observed and discussed in other amphibole compositions by Robert *et al.* (1999, 2000) and Della Ventura *et al.* (2014), who interpreted this shift on the basis of the presence of the $^{O(3)}$OH–^{A}Na–$^{O(3)}$F local arrangement. In tremolite, the local arrangement MgMgMg–OH–$^{A}\square$:SiSi (the band occurring at 3672 cm^{-1}) could also generate a band at 3658 cm^{-1} due to $^{O(3)}$OH–^{A}Na–$^{O(3)}$F local order.

The FTIR spectrum of fluoro-tremolite in the range from 1200 to 400 cm^{-1} is very similar to the spectrum of synthetic fluoro-tremolite described in Ishida *et al.* (2008), who ascribed region 1 to Si–O stretching vibrations, and region 2 mainly to Si–O–Si and O–Si–O deformation, except for the band at 687 cm^{-1} that can be assigned to the O–H libration. The strong band at 509 cm^{-1} and its pronounced shoulder at 544 cm^{-1} are due to M–O (M = Mg, Ca, Na, Si and Al)

deformations (Lazarev, 1972; Strens, 1974; Ishida, 1990; Andrut *et al.*, 2000; Ishida *et al.*, 2008).

Acknowledgements

The authors are grateful to Frank Hawthorne and Andrew Locock, who provided careful reviews of the manuscript.

Supplementary material

To view supplementary material for this article, please visit https://doi.org/10.1180/minmag.2017.081.029

References

Andrut, M., Gottschalk, M., Melzer, S. and Najorka, J. (2000) Lattice vibrational modes in synthetic tremolite-Sr-tremolite and tremolite-richterite solid solutions. *Physics and Chemistry of Minerals*, **27**, 301–309.

Bruker (2003) *SAINT Software Reference Manual. Version 6*. Bruker AXS Inc., Madison, Wisconsin, USA.

Burke, E.A. and Leake, B.E. (2004) "Named amphiboles": a new category of amphiboles recognized by the International Mineralogical Association (IMA), and the proper order of prefixes to be used in amphibole names. *Canadian Mineralogist*, **42**, 1881–1884.

Burns, R.G. and Strens, R.G. (1966) Infrared study of the hydroxyl bands in clinoamphiboles. *Science*, **153**, 890–892.

Cameron, M. and Gibbs, G.V. (1973) The crystal structure and bonding of fluor-tremolite: A comparison with hydroxyl tremolite. *American Mineralogist*, **58**, 879–888.

Dachs, E., Baumgartner, I.A., Bertoldi, C., Benisek, A., Tippelt, G. and Maresch, W.V. (2010) Heat capacity and third-law entropy of kaersutite, pargasite, fluor-opargasite, tremolite and fluorotremolite. *European Journal of Mineralogy*, **22**, 319–331.

Della Ventura, G., Bellatreccia, F., Cámara, F. and Oberti, R. (2014) Crystal-chemistry and short-range order of fluoro-edenite and fluoro-pargasite: a combined X-ray diffraction and FTIR spectroscopic approach. *Mineralogical Magazine*, **78**, 293–310.

Gunter, M.E., Downs, R.T., Bartelmehs, K.L., Evans, S. H., Pommier, C.J.S., Grow, J.S., Sanchez, M.S. and Bloss, F.D. (2005) Optic properties of centimeter-sized crystals determined in air with the spindle stage using EXCALIBRW. *American Mineralogist*, **90**, 1648–1654.

Hawthorne, F.C. and Della Ventura, G. (2007) Short-range order in amphiboles. Pp. 173–222 in: *Amphiboles: Crystal Chemistry, Occurrence and Health Issues* (F.C. Hawthorne, R. Oberti, G. Della Ventura and A. Mottana, editors). Reviews in Mineralogy & Geochemistry, **67**. The Mineralogical Society of America and the Geochemical Society, Chantilly, Virginia, USA.

Hawthorne, F.C. and Grundy, H.D. (1976) The crystal chemistry of the amphiboles: IV. X-ray and neutron refinement of the crystal structure of tremolite. *Canadian Mineralogist*, **14**, 334–345.

Hawthorne, F.C., Della Ventura, G. and Robert, J.-L. (1996) Short-range order of (Na,K) and Al in tremolite: An infrared study. *American Mineralogist*, **81**, 782–784.

Hawthorne, F.C., Welch, M.D., Della Ventura, G., Liu, S., Robert, J.-L. and Jenkins, D.M. (2000) Short-range order in synthetic aluminous tremolites: An infrared and triple-quantum MAS NMR study. *American Mineralogist*, **85**, 1716–1724.

Hawthorne, F.C., Oberti, R., Harlow, G.E., Maresch, W.V., Martin, R.F., Schumacher, J.C. and Welch, M.D. (2012) Nomenclature of the amphibole supergroup. *American Mineralogist*, **97**, 2031–2048.

Höpfner, J.G.A. (1789) I. Uber die Klassifikation der Fossilien in einem Schreiben des Herausgebers an Herrn Dr. Karsten in Halle. II. "Versuch einer neuen Classifikationsmethode der Stein- und Erdarten, nach den neuesten chemischen Erfahrungen". *Magazin für die Naturkunde Helvetiens*, **4**, 255–332.

Ishida, K. (1990) Identification of infrared OH librational bands of talc–willemseite solid solutions and AlIV-free amphiboles through deuteration. *Mineralogical Journal*, **15**, 93–104.

Ishida, K., Jenkins, D.M. and Hawthorne, F.C. (2008) Mid-IR bands of synthetic calcic amphiboles of tremolite-pargasite series and of natural calcic amphiboles. *American Mineralogist*, **93**, 1112–1118.

Lazarev, A.N. (1972) *Vibrational Spectra and Structure of Silicates*. Consultants Bureau, New York, p. 302.

Mandarino, J.A. (1981) The Gladstone-Dale relationship: Part lV. The compatibility concept and its application. *Canadian Mineralogist*, **19**, 441–450.

Oberti, R., Hawthorne, F.C., Cannillo, E. and Cámara, F. (2007) Long-range order in amphiboles. Pp. 125–172 in: *Amphiboles: Crystal Chemistry, Occurrence and Health Issues* (F.C. Hawthorne, R. Oberti, G. Della Ventura and A. Mottana editors). Reviews in Mineralogy & Geochemistry, **67**. The Mineralogical Society of America and the Geochemical Society, Chantilly, Virginia, USA.

Papike, J.J., Ross, M. and Clark, J.R. (1969) Crystal-chemical characterization of clinoamphiboles based on five new structure refinements. *Mineralogical Society of America Special Paper*, **2**, 117–136.

Petersen, E.U., Essene, E.J., Peacor, D.R. and Valley, J.W. (1982) Fluorine endmember micas and amphiboles. *American Mineralogist*, **67**, 538–544.

Pouchou, J.L. and Pichoir, F. (1985) 'PAP' (φρZ) procedure for improved quantitative microanalysis. Pp. 104–160 in: *Microbeam Analysis* (J.T. Armstrong, editor). San Francisco Press, San Francisco, California, USA.

Robert, J.-L., Della Ventura, G. and Hawthorne, F.C. (1999) Near-infrared study of short-range disorder of OH and F in monoclinic amphiboles. *American Mineralogist*, **84**, 86–91.

Robert, J.-L., Della Ventura, G., Welch, M. and Hawthorne, F. C. (2000) OH-F substitution in synthetic pargasite at 1.5 kbar, 850°C. *American Mineralogist*, **85**, 926–931.

Shannon, R.D. (1976) Revised effective ionic radii and systematic studies of interatomic distances in halides and chalcogenides. *Acta Crystallographica*, **A32**, 751–767.

Strens, R.G.J. (1974) The common chain, ribbon, and ring silicates. Pp. 305–330 in: *The Infra-Red Spectra of Minerals* (V.C. Farmer, editor). Mineralogical Society, London.

Su, S.C., Bloss, F.D. and Gunter, M.E. (1978) Procedures and computer programs to refine the double variation method. *American Mineralogist*, **72**, 1011–1013.

Valley, J.W., Petersen, E.U., Essene, E.J. and Bowman, J. R. (1982) Fluorphlogopite and fluortremolite in Adirondack marbles and calculated C-O-H-F fluid compositions. *American Mineralogist*, **67**, 545–557.

Warren, B.E. (1929) The structure of tremolite $H_2Ca_2Mg_5(SiO_3)_8$. *Zeitschrift für Kristallographie* **72**, 42–57.